

T-cell receptor repertoire analysis of CD4-positive T cells from blood and an affected organ in an autoimmune mouse model

Tatsuya Ishikawa^{1,2} | Kenta Horie¹ | Yuki Takakura¹ | Houko Ohki^{1,2} |
 Yuya Maruyama^{1,2} | Mio Hayama^{1,2} | Maki Miyauchi^{1,2} | Takahisa Miyao^{1,2} |
 Naho Hagiwara¹ | Tetsuya J. Kobayashi³ | Nobuko Akiyama^{1,2} |
 Taishin Akiyama^{1,2} 

¹Laboratory of Immune Homeostasis, RIKEN Center for Integrative Medical Sciences, Yokohama, Japan

²Graduate School of Medical Life Science, Yokohama City University, Yokohama, Japan

³Institute of Industrial Science, The University of Tokyo, Tokyo, Japan

Correspondence

Nobuko Akiyama and Taishin Akiyama, Laboratory of Immune Homeostasis, RIKEN Center for Integrative Medical Sciences, Yokohama, Japan.

Email: nobuko.akiyama@riken.jp and taishin.akiyama@riken.jp

Funding information

Core Research for Evolutional Science and Technology, Grant/Award Number: JPMJCR2011; Japan Society for the Promotion of Science, Grant/Award Numbers: 20H03441, 20K07332; Japan Science and Technology Agency, Grant/Award Number: JPMJFS2140

Communicated by: Sho Yamasaki

Abstract

One hallmark of some autoimmune diseases is the variability of symptoms among individuals. Organs affected by the disease differ between patients, posing a challenge in diagnosing the affected organs. Although numerous studies have investigated the correlation between T cell antigen receptor (TCR) repertoires and the development of infectious and immune diseases, the correlation between TCR repertoires and variations in disease symptoms among individuals remains unclear. This study aimed to investigate the correlation of TCR α and β repertoires in blood T cells with the extent of autoimmune signs that varies among individuals. We sequenced TCR α and β of CD4⁺CD44^{high}CD62L^{low} T cells in the blood and stomachs of mice deficient in autoimmune regulator (*Aire*) (AIRE KO), a mouse model of human autoimmune polyendocrinopathy-candidiasis-ectodermal dystrophy. Data analysis revealed that the degree of similarity in TCR sequences between the blood and stomach varied among individual AIRE KO mice and reflected the extent of T cell infiltration in the stomach. We identified a set of TCR sequences whose frequencies in blood might correlate with extent of the stomach manifestations. Our results propose a potential of using TCR repertoires not only for diagnosing disease development but also for diagnosing affected organs in autoimmune diseases.

KEYWORDS

AIRE, autoimmunity, T cells, TCR repertoire

1 | INTRODUCTION

Autoimmune diseases result from disrupted immune systems that trigger inflammation against various organs. Some autoimmune diseases present highly heterogeneous

symptoms, as the severity and affected organs vary among patients. For example, systemic lupus erythematosus can affect various organs, including joints, skin, kidneys, heart, the hematopoietic system, and the nervous system, but with varying degrees of involvement among

patients (Allen et al., 2021; Wu et al., 2017). This individual variation is also seen in patients with APECED. APECED is caused by loss-of-function mutations in *AIRE*, a gene encoding the nuclear factor responsible for ectopic expression of peripheral-tissue antigens by thymic epithelial cells to mediate negative selection of self-reactive thymocytes in the thymus (Anderson et al., 2002; Perniola, 2018). Patients are diagnosed as APECED by developing at least two symptoms among endocrine deficiency, ectodermal dystrophy, and chronic mucocutaneous candidiasis (Betterle et al., 1998; Perheentupa, 1996). While some organs, such as adrenal and parathyroid glands, are constantly affected, others like thyroid glands and the pancreas are affected in only 2%–12% of cases, and gastritis is seen in 13%–15% of cases (Betterle et al., 1998; Perheentupa, 1996).

Mice deficient in *Aire* (AIRE KO) were previously established and showed autoimmune phenotypes (Anderson et al., 2002; Goldfarb et al., 2021; Hubert et al., 2009; Jiang et al., 2005; Niki et al., 2006; Ramsey et al., 2002; Su et al., 2008; Venanzi et al., 2008). Analysis of these mutant mice revealed that AIRE regulates thousands of tissue specific antigens (TSAs) in medullary thymic epithelial cells (mTECs). mTECs express and present these TSAs, thereby promoting negative selection of TSA-reactive T cells and generation of regulatory T cells in the thymus.

While autoimmune phenotypes in AIRE knockout (KO) mice were reported to be independent of microorganisms and their derivatives (Gray et al., 2007), the severity of symptoms, as well as the organs affected, can vary among different genetic backgrounds (Jiang et al., 2005; Niki et al., 2006), types of mutations (Goldfarb et al., 2021; Hubert et al., 2009; Kuroda et al., 2005; Su et al., 2008), and individuals (Anderson et al., 2002; Jiang et al., 2005; Ramsey et al., 2002; Venanzi et al., 2008). In addition to these deterministic factors, this variation may be ascribed partly to the stochastic nature of TSA expression regulated by AIRE (Dhalla et al., 2020; Meredith et al., 2015), and to the inherent stochasticity that thymic T cells need to encounter mTECs, which are a rare population among total thymic cells, for thymic selection.

Because of the heterogeneous nature of autoimmune diseases, diagnosis of affected organs is necessary. In addition to the approach by detecting organ-specific protein markers (Suzuki et al., 2008; Zhang et al., 2023) (e.g., Neurofilament light chain in multiple sclerosis), it would be desirable to be able to use TCR repertoire analysis for diagnosis. TCR repertoire is formed by a combination of the hypervariable complementarity-determining region 3 (CDR3) loop of TCRs on their cell membranes and diverse V(D)J recombination in the

thymus, allowing T cells to recognize myriad antigens in the body (Schatz & Ji, 2011). Since T cells play critical roles in development of autoimmune diseases by recognizing self-antigens, their TCR repertoires change depending on affected organs (Mitchell & Michels, 2020). Therefore, diagnosis by detecting their TCR repertoires prior to disease exacerbation may provide an earlier window for disease diagnosis than the approach detecting organ-specific protein markers. For example, by using peripheral blood samples from patients, multiple studies have shown altered utilization of V and J genes in patients with systemic lupus erythematosus, rheumatoid arthritis, and Sjogren's syndrome (Liu et al., 2019; Lu et al., 2022; Ye et al., 2020). Moreover, Moore et al. have performed TCR repertoire analyses of spleen, salivary gland, and brain choroid plexus from an MRL/lpr mouse model of lupus and identified a set of TCR sequences significantly detected in the brain (Moore et al., 2020). However, despite growing evidence suggesting a correlation between TCR repertoires and development of autoimmune diseases, the correlation between TCR repertoires and variations in disease severity of autoimmune diseases has rarely been studied.

In the present study, we performed TCR α and β sequencing in the blood and stomachs of Aire-deficient mice (AIRE KO), a mouse model of APECED. The data suggest that some TCR repertoires in the blood and stomach were commonly increased in these mice and correlated with the extent of T cell infiltration in the stomach. This finding supports the diagnostic potential of TCR repertoire in monitoring the onset and affected organs of autoimmune diseases.

2 | RESULTS

2.1 | Individual variation in phenotypes of AIRE KO mice

Our aim in this study was to seek the correlation of TCR sequence with the extent of autoimmune manifestations in a murine model. As a murine model of autoimmune diseases, we chose gastric autoimmunity of AIRE KO mice because: (1) the stomach is large enough to obtain sufficient numbers of T cells for TCR sequencing and (2) autoimmune inflammation in the stomach is heterogeneously induced in AIRE KO mice (Anderson et al., 2002; Jiang et al., 2005).

We first confirmed the heterogeneous features of autoimmune phenotypes in the stomachs of AIRE KO mice. Inflammatory status of the stomachs was evaluated for AIRE KO mice approximately 30 weeks old and their wild-type littermates (AIRE WT) as controls. Flow

cytometric analysis indicated that the proportion and cell numbers of CD44^{high}CD62L^{low} activated effector memory T cells (Teffs) among CD4⁺ and CD8⁺ T cells were significantly increased compared to controls (Figure 1a,b; Figure S1), manifesting stomach inflammation with activated T cell infiltration in mutant mice. In contrast, the frequency of Foxp3⁺CD25⁺ was not changed in the stomach and blood of AIRE KO mice compared to AIRE WT (Figure S2).

We further evaluated generation of autoantibodies against stomach tissues by immunohistochemical staining of the stomach section from RAG1-deficient

(*Rag1*^{-/-}) mice with serum of AIRE KO mice (Figure 1c, left). Quantification of these immunofluorescent images showed that the level of autoantibodies against the stomach was significantly higher in the serum of AIRE KO mice than that of AIRE WT mice (Figure 1c, right), which is consistent with previous studies (Gavanescu et al., 2007). Notably, standard deviations (SD) in the number of CD4⁺ Teffs and serum levels of anti-stomach antibodies are higher in AIRE KO mice than in controls (Figure 1a–c, SD = 27,780 and 7076 each for the CD4⁺ Teff number and SD = 17,061 and 614 for the CD8⁺ Teff number in AIRE KO and control mice, respectively;

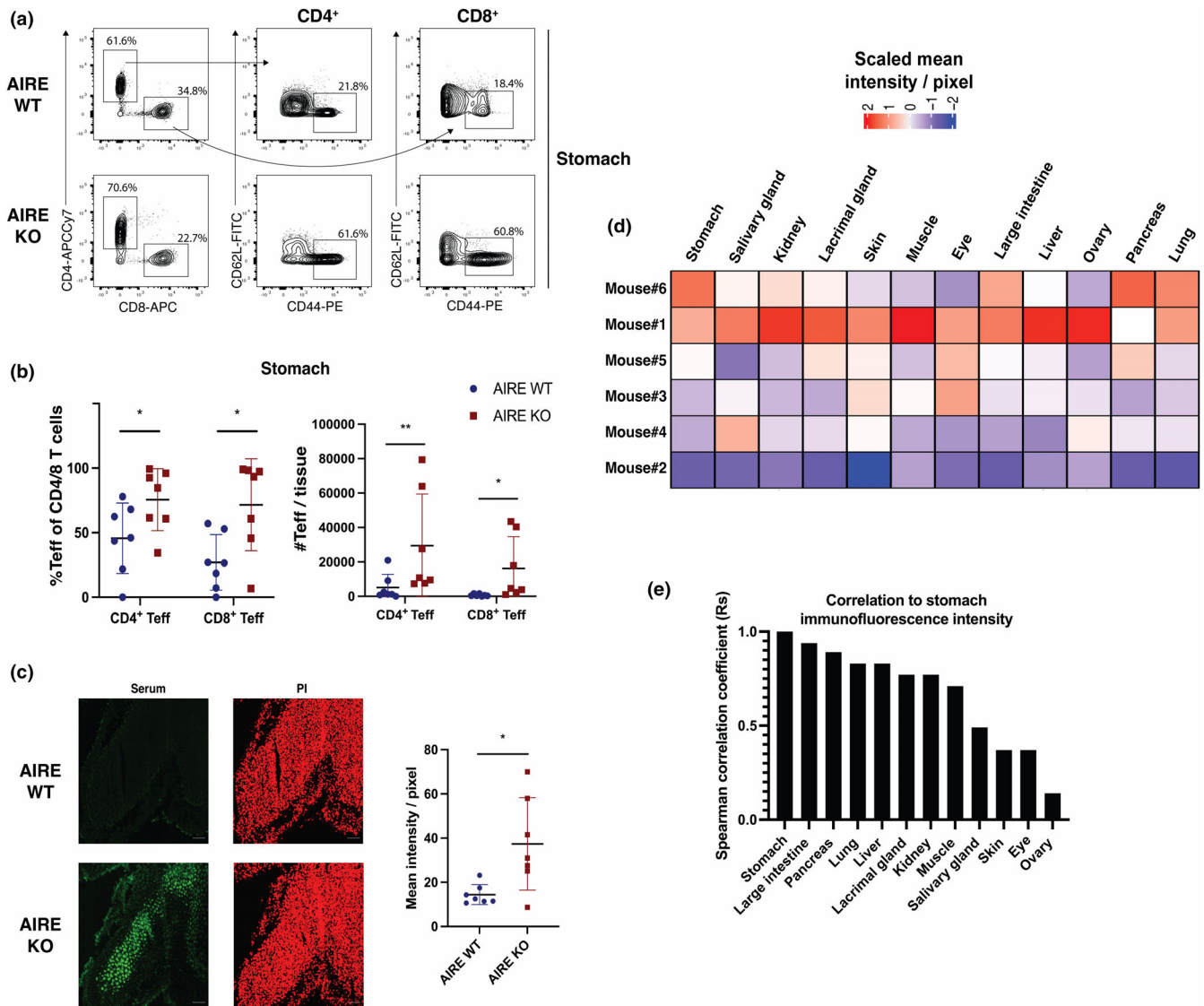


FIGURE 1 Individual variation in multi-organ phenotypes of AIRE KO mice. (a) Flow cytometric analysis of CD4⁺ and CD8⁺ Teffs from stomachs of AIRE WT and AIRE KO mice. (b) Numbers and percentages of CD4⁺ and CD8⁺ Teffs from stomachs of AIRE WT and AIRE KO mice. Two-tailed Student's *t*-test and Mann–Whitney *U* test were used for statistical analyses of the cell number and the percentage, respectively. (c) Immunofluorescent staining of AIRE WT and AIRE KO sera against stomach sections of *Rag1*^{-/-} mice. Data were analyzed using Mann–Whitney *U* test. (d) Heatmap of scaled mean intensity of immunofluorescent signals. (e) Spearman correlation coefficients (Rs) between stomach immunofluorescence signals and those of other organs. ns, not significant (*p* > .05). **p* < .05; ***p* < .01.

SD = 19.3 and 4.17 each for the serum antibody level in AIRE KO and control mice, respectively). Thus, there was large variation among individual AIRE KO mice in the number of infiltrated Teffs in the stomach and serum levels of anti-stomach antibodies. Consequently, significant individual variation in stomach manifestations was confirmed in this line of AIRE KO mice.

Dysfunction of AIRE provokes autoimmunity targeting multiple organs. We next investigated how the extent and target organs of autoimmunity vary in this Aire-deficient mice line from individual to individual. Titers of autoantibodies to various organs in the serum were quantified by immunohistochemical staining (Figure S3). These results showed that the profile of targeted organs varied markedly among individual mice (Figure 1d,e). Mouse #1 was the most severely affected, as it produced the broadest profile with the greatest number of organs having high autoantibody signal intensity. On the other hand, Mouse #6 showed a sporadic profile with the highest signal intensity for the stomach, lung, and pancreas. Mice #3, #4, and #5 also produced sporadic profiles with relatively high intensity for organs such as skin, eyes, and salivary glands. Finally, Mouse #2 produced the smallest signal in the greatest number of organs examined. We also evaluated the correlation of autoantibody signal intensity of stomach with that of other organs. While organs such as large intestine, pancreas, and lung showed high correlation, skin, eyes, and ovaries showed low correlation with stomachs, suggesting that titers of serum autoantibodies against each tissue vary among individuals in these AIRE KO mice (Figure 1d,e). Taken together, these results indicate that autoimmune phenotypes of AIRE KO mice used in this study are heterogeneous. Accordingly, AIRE KO mice can comprise a model to assess the potential of TCR repertoires to monitor disease onset and affected organs.

2.2 | Limited correlation of blood T cell count, TCR diversity, clonality, CDR3 length, and V/J usage with disease severity in AIRE KO mice

Before performing TCR sequencing, we asked whether blood T cell counts might reflect the onset of autoimmunity in AIRE KO mice. To this end, we used flow cytometry to detect CD4⁺ and CD8⁺ Teffs in the blood of AIRE KO and AIRE WT mice. We found that both the proportion and the number of CD4⁺ and CD8⁺ Teffs were comparable in AIRE KO and AIRE WT mice (Figure 2a,b). Thus, the Teff count in blood does not reflect the onset of autoimmunity in AIRE KO mice.

For TCR sequencing analysis, we sorted CD4⁺ Teffs in the blood and stomach (Table S1) because autoimmune phenotypes of AIRE KO are predominantly B-cell mediated (Gavanescu et al., 2008). Approximately 5000 to 15,000 CD4⁺ Teffs were FACS-sorted from the blood of WT (Blood WT) and AIRE KO (Blood KO). For the stomach, all CD4⁺ Teffs present in the organ were sorted. The total number of CD4⁺ Teffs obtained from the AIRE KO stomach (Stomach KO) ranged from 2000 to 40,000 per stomach (hereafter referred to as stomach Teff count). The CD4⁺ Teff number in the WT stomach was too low to be used for TCR sequencing. Total RNA of these sorted CD4⁺ Teffs was prepared successfully from six AIRE KO (labeled from #1–6) and 7 AIRE WT (labeled from #7–13) mice with sufficient quality for TCR sequencing. Of note, the stomach Teff count showed a weak correlation with the fluorescence intensity of stomach immunostaining, which reflects the titer of autoantibodies in the serum (Figure 2c, $R_s = 0.77$, $p = .10$). In contrast, as expected, there was no correlation between the number of blood CD4⁺ ($R_s = 0.37$, $p = .56$) or CD8⁺ Teffs ($R_s = 0.37$, $p = .50$) with the mean signal intensity of stomach immunofluorescence (Figure 2d).

We performed TCR repertoire sequencing of these sorted CD4⁺ Teffs (Table S1). To consider the difference in cell number, the amount of RNA extracted from each sample was normalized for cDNA library preparation. By analyzing sequencing data, some parameters of TCR α and β repertoires such as diversity, clonality, CDR3 length, and V/J usage, were determined in each sample. We then sought to find parameters that predict disease onset in the stomachs of these AIRE KO mice according to two criteria: (1) the difference between Blood KO and Blood WT, for prediction by measurement of blood TCR repertoires, and (2) the similarity between Blood KO and Stomach KO, for supporting the reflection of stomach manifestations.

First, we calculated the number of unique clonotypes and normalized Shannon indices to evaluate diversity and clonality, respectively, of TCRs from Blood WT, Blood KO, and Stomach KO. We found that diversity among Blood WT, Blood KO, and Stomach KO was comparable for both TCR α and β (Figure 3a). Chao1, another diversity index, was also comparable among all groups for both TCR α and TCR β (Figure S4). On the other hand, we found that TCR α clonality was significantly increased in Stomach KO in the Shannon index (Figure 3a) while TCR β clonality was comparable among all groups. Consistently, the Inverse Simpson index was high for TCR α in Stomach KO (Figure S4) and that of TCR β was relatively comparable among all groups. Overall, the diversity is comparable in both TCR α and TCR β in AIRE KO

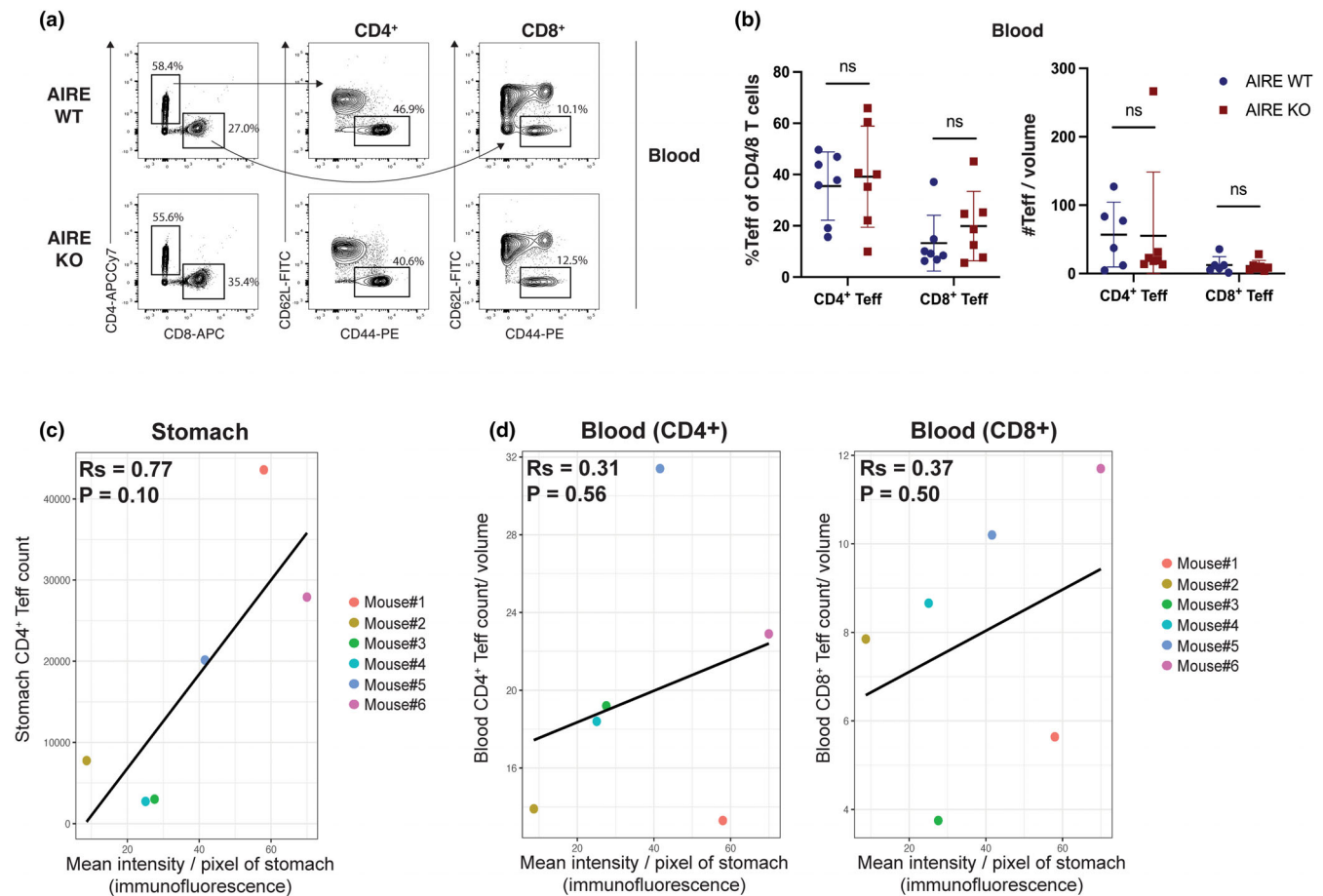


FIGURE 2 Correlation of activated T cell number in the stomach and blood with titer of anti-stomach antibody in AIRE KO mice. (a) Flow cytometric analysis of CD4⁺ and CD8⁺ Tregs from the blood of AIRE WT and AIRE KO mice. (b) Numbers and percentages of CD4⁺ and CD8⁺ Tregs from the blood of AIRE WT and AIRE KO mice. Two-tailed Student's *t*-test and Mann–Whitney *U* test were used for statistical analyses of the cell number and the percentage, respectively. (c) Spearman's correlation of stomach CD4⁺ Treg count with mean signal intensity of stomach immunofluorescence, reflecting the titer of anti-stomach antibody. (d) Spearman's correlation of blood CD4⁺ Tregs (left) or CD8⁺ Tregs (right) with the mean signal intensity of stomach immunofluorescence. *R*_s, Spearman's correlation coefficient. *P*, *p* value determined from Spearman's correlation.

whereas TCR α clonality of Stomach KO is higher as compared to that of blood samples.

Similar to clonality, the amino acid length of CDR3 significantly decreased in Stomach KO for TCR α but remained comparable among all groups for TCR β (Figure 3b). Similar CDR3 length distributions following a Gaussian pattern were also observed in T cells from diseased organs in other mouse models of autoimmune disease (Moore et al., 2020). Although there were slight changes in amino acid usage at each position of CDR3 in Stomach KO compared to blood samples, no clear trend emerged (Figure S4c). In support of the trend of clonality and CDR3 length, most significantly detected V and J genes were strongly present in Stomach KO for TCR α , but were comparably present in all groups for TCR β (Figure 3c–e). Since diversity, clonality, CDR3 length, and V/J usage for TCR α and β repertoires did not meet

criteria for correlation, we concluded that these measures do not reflect disease severity in AIRE KO.

2.3 | Individual similarities of TCR repertoires in the blood and stomachs of AIRE KO

We then shifted our attention to individual sequences in TCR α and β chains and focused on shared TCR sequences of CD4⁺ Tregs in the blood and stomach from the same AIRE KO mice. To this end, we calculated Jaccard indices to evaluate the similarity of TCR α and β repertoires based on the proportion of shared TCR sequences between each paired blood (Blood#1–13) and stomach sample (Stomach #1–6). Scatterplots and heat maps of Jaccard indices suggested that Blood KO

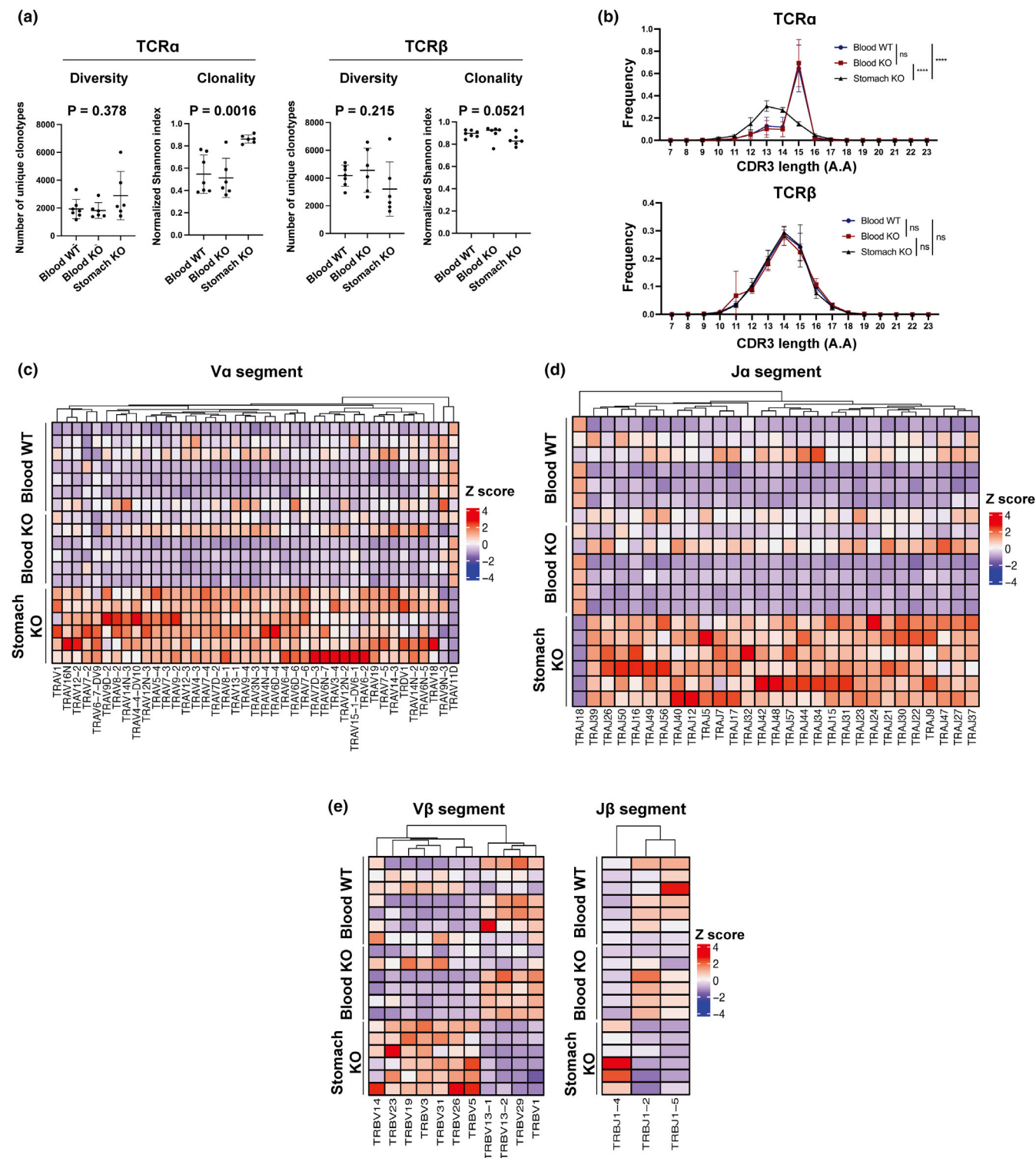


FIGURE 3 TCR repertoire analysis of blood and stomachs of AIRE KO mice. (a) Diversity and clonality of TCR α and β of Blood WT, Blood KO, and Stomach KO. Kruskal–Wallis test was used for comparisons and its p value, P , is shown. (b) CDR3 amino acid length distributions of TCR α and β of Blood WT, Blood KO, and Stomach KO. Two-way ANOVA with random variables. **** $p < .0001$. ns, not significant ($p > .05$). Heatmap showing scaled frequencies of significantly detected V α (c), J α (d), V β , and J β (e) genes between Blood WT and Blood KO and between Stomach KO and Blood WT/KO.

correlated with the corresponding Stomach KO (Figure 4a,b; Tables S2 and S3). Indeed, Jaccard indices of the blood and stomach from the same AIRE KO mice

(on average about 4%) were four times higher than those of blood and stomachs from different mice (on average about 1%) for both TCR α and β (Figure 4c). Thus, TCR α

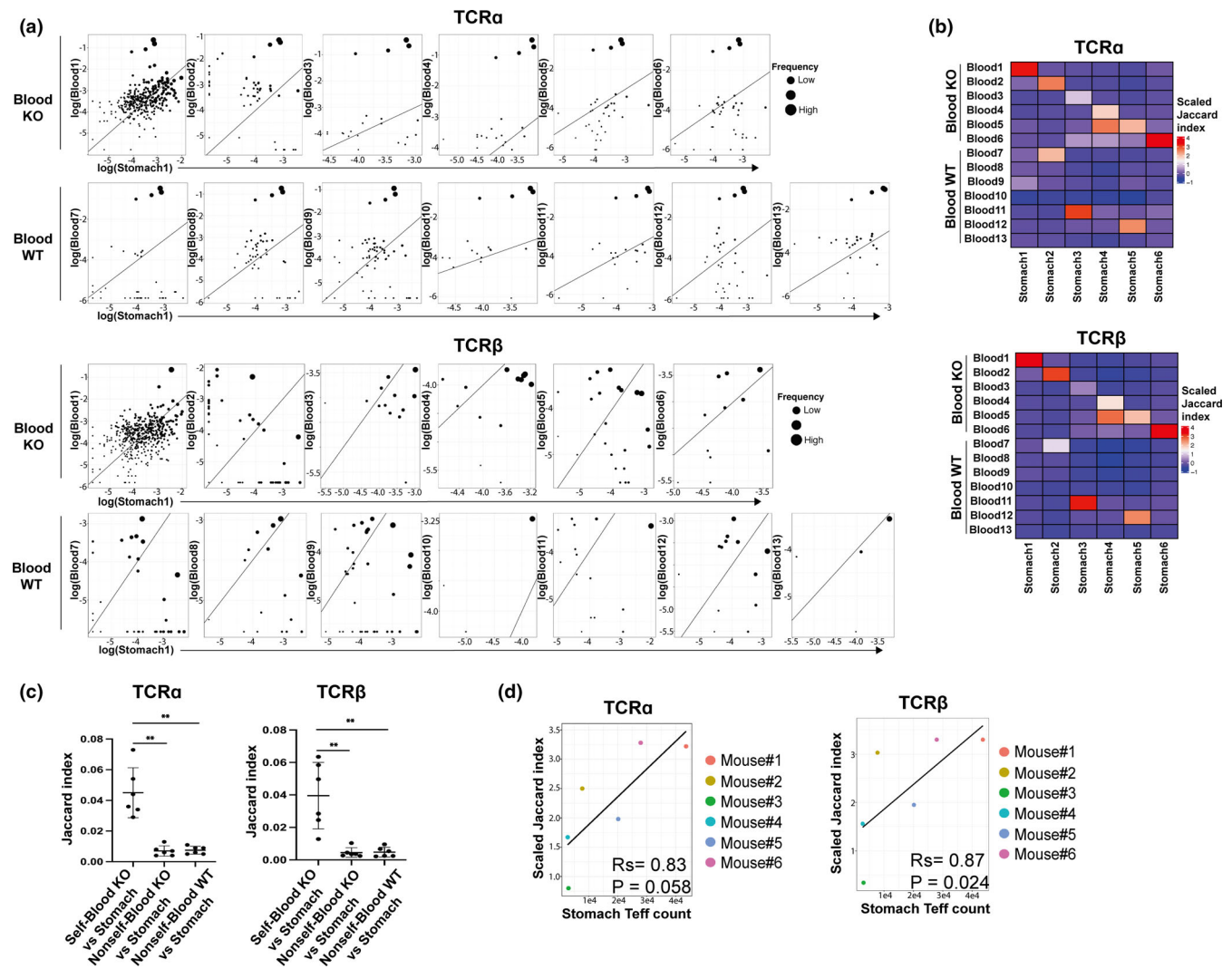


FIGURE 4 Individual similarity of TCR repertoires between blood and stomachs of AIRE KO. (a) Scatterplot showing frequencies of TCRs shared between Stomach 1 and each of the blood samples. (b) Heatmap of scaled Jaccard indices of each of blood and stomach pair. (c) Self-Blood KO vs Stomach: Jaccard indices of the stomach and blood from the same AIRE KO mice are plotted. Nonsel-Blood KO versus Stomach: For each AIRE KO mice, average Jaccard indices of the stomach and blood from different AIRE KO mice are plotted. Nonsel-Blood KO versus Stomach: For each AIRE KO mice, average Jaccard indices of the stomach and blood from AIRE WT mice are plotted. Mann–Whitney U test. $**p < .01$. (d) Spearman's correlation between stomach Teff counts and scaled Jaccard indices of the blood and stomach from each AIRE KO mouse (from #1 to #6). R_s , Spearman's correlation coefficient.

and β repertoires in the blood correlate with those in the stomach repertoire of AIRE KO mice, and more importantly, the correlation of each TCR repertoire between stomach and blood is individualized. Notably, scaled Jaccard indices correlated with the stomach Teff count, a measure reflecting the severity of the stomach manifestation (Figure 4d, $p = .058$ for TCR α and $p = .024$ for TCR β). Thus, mice with more severe gastric inflammation may have more common TCR repertoires in blood and stomach. Overall, these data support the potential for monitoring the severity of stomach manifestation by detecting TCR sequences common to the blood and stomach in AIRE KO.

2.4 | Identification of candidate TCR α and β repertoires to monitor disease severity in AIRE KO

We next sought to determine sequences of TCR α and β repertoires in CD4⁺ Teffs that correlate with Stomach CD4⁺ Teff count. Such TCR repertoires could monitor the severity of stomach manifestations in AIRE KO mice as a biomarker. To this end, we first screened the CDR3 of TCR sequences according to three criteria: (1) CDR3 sequences that were detected in both the Stomach KO and Blood KO of the same mice, (2) were found in at least two AIRE KO mice, and (3) were not present in

Blood WT. As a result, we successfully identified 29 CDR3 sequences for both TCR α and β . We then categorized these CDR3 sequences based on their amino acid sequences using the *tcrdist3* package to assign mismatch distance between two CDR3 sequences based on the BLOSUM62 substitution matrix (Dash et al., 2017). The matrix gives the score that determines whether an amino acid substitution is conservative or nonconservative, reflecting the similarity of biochemical properties of two amino acids. The distance matrix was then used for hierarchical clustering. Based on the clustering result, we categorized identified CDR3 amino acid sequences into four clusters (k -means = 4) for TCR α (Figure 5a) and three clusters (k -means = 3) for TCR β (Figure 5b).

Since a biomarker should discriminate between diseased and non-diseased subjects, we searched for clusters containing CDR3 sequences whose frequencies from the blood and stomach correlated with the severity of stomach manifestations, represented by the stomach Teff count. We found that the mean frequencies of CDR3 sequences classified as Cluster3 in TCR α and classified as Cluster1 in TCR β (hereafter referred to as Cluster3/TCR α and Cluster1/TCR β , respectively) showed some positive correlation with both the blood and stomach ($R_s > 0.5$) (Figure 5c,d; Figure S5). Stomach TCR frequencies of Cluster 3/TCR α and Cluster1/TCR β were able to discriminate the two mice with the highest stomach Teff counts (Mouse #1 and Mouse #6) from the other mice. However, blood TCR frequencies of these clusters were not clearly correlated with stomach Teff counts (Figure 5c–f). Especially for Cluster1/TCR β , high TCR frequencies in the stomach of Mouse #6 were not reflected in the blood (Figure 5d,f). Therefore, we focused on Cluster3/TCR α and found that when we divided Cluster3 into two sub-clusters, Clusters 3.1 and 3.2 (Figure 5g), TCR frequencies of Cluster 3.1 were relatively high in the blood of Mouse #2 (Figure 5e,h; Table S4), a mouse with a low stomach Teff count (Figure 5h). By contrast, TCR frequencies of Cluster 3.2 showed a relatively strong correlation with stomach Teff counts for both the blood ($R_s = 0.64$) and stomach ($R_s = 0.64$) (Figure 5h). Therefore, we used the TCR frequencies of Cluster 3.2 from the blood or stomach and finally confirmed their correlations with two distinct dimensions reflecting the severity of stomach manifestations, stomach Teff count and mean signal intensity in immunofluorescent staining of the stomach (Figure 5i). The result of 3D plots showed that by using TCR frequencies of Cluster 3.2 from both the blood and stomach, Mouse #1 and Mouse #6 are clearly distinguished from the others.

3 | DISCUSSION

In the present study, we used an AIRE KO mouse model of APECED to test whether TCR repertoires can serve as biomarkers to monitor organ manifestations in autoimmune disease. We proposed a set of TCR sequences in Cluster 3.2 of TCR α that may discriminate mice with relatively severe autoimmunity from other mice. These data support the potential of TCR repertoires to monitor disease severity, at least in this AIRE KO mouse model of autoimmune disease. However, it should be noted that there were relatively large individual differences in the experimental data for CD4⁺ Teff in the stomach and blood. These differences may be due to inherent variation among individuals, as well as slight differences in the rearing environment, such as food accessibility. To address these issues, it will be crucial to collect data from a larger number of samples and to analyze T cells obtained from additional organs in the future.

A previous study suggested that hydrophobic amino acid residues are enriched in CDR3 region of the TCR β chain in self-reactive T cells (Stadinski et al., 2016). However, we did not observe a similar trend among all samples, including Stomach KO, which would be expected to have an enrichment of activated self-reactive T cells. Instead, our data revealed significant alterations in the clonality, CDR3 length, and V/J usage of Stomach KO repertoires for TCR α as compared to those of Blood WT and Blood KO, while the changes in TCR β repertoires were less pronounced. The reason for the preferential change in TCR α over TCR β should be clarified in the future. On the other hand, we found no significant differences in diversity, clonality, CDR3 length, or V/J usage between Blood WT and Blood KO. This aligns with a previous study demonstrating comparable TCR repertoire diversity in the blood of AIRE WT and AIRE KO mice (Ofteidal et al., 2017).

To date, most analyses of TCR repertoire in autoimmune diseases have been conducted to monitor disease development rather than variation in disease manifestations (Mitchell & Michels, 2020). Most previous studies simply compared TCR repertoires between patients and normal individuals and searched for common TCR sequences that were abundant in patients (Liu et al., 2019; Lu et al., 2022; Ye et al., 2020). In addition to our current study, further investigations would be necessary to address the potential of TCR repertoires to dissect disease heterogeneity.

Despite the identification of candidate TCR repertoires to monitor stomach manifestation in AIRE KO mice, there is no guarantee that these TCR repertoires specifically recognize a self-antigen derived from the stomach. To address

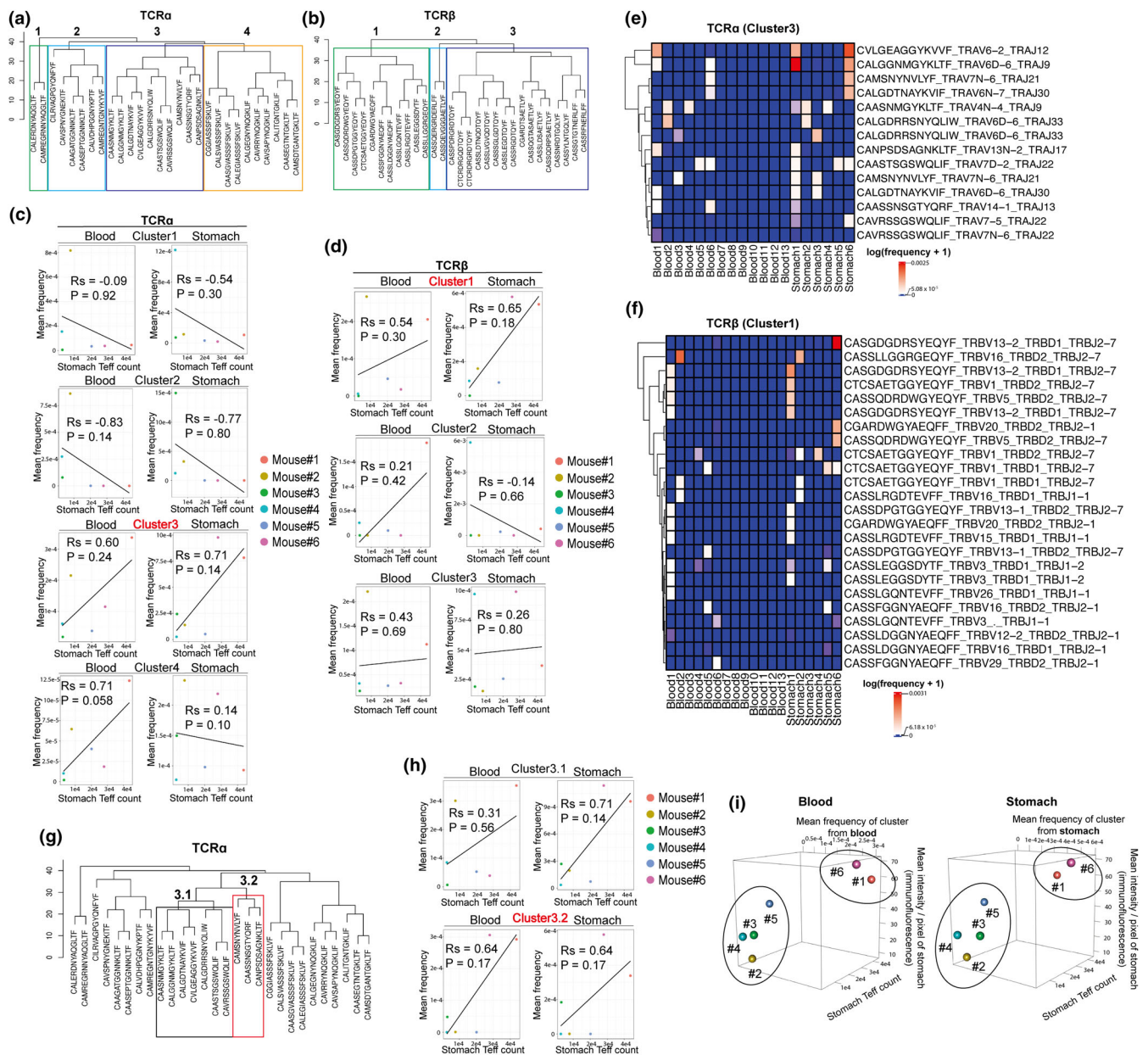


FIGURE 5 Identification of candidate TCR repertoires correlating with severity of stomach manifestation in AIRE KO. Hierarchical clustering of candidate TCRα (a) and β (b) repertoires. Cluster numbers are shown at the tops of trees. Spearman's correlation of stomach CD4⁺Teff counts and mean frequencies of TCRα (c) and β (d) sequences contained in each cluster detected in the blood (left) and stomach (right) of each AIRE KO mouse. Heatmap showing log-transformed frequencies of TCRα sequences contained in Cluster3 (e) and TCRβ sequences contained in Cluster1 (f). Different CDR3 nucleotide sequences encoding the same CDR3 amino acid sequences are also shown in the heatmap. (g) Hierarchical clustering tree showing subclusters of Cluster3 of TCRα (Cluster3.1 and 3.2). (h) Spearman's correlation of stomach CD4⁺Teff counts and mean frequencies of TCRα sequences in Clusters 3.1 (top) and 3.2 (bottom) detected in the blood (left) and stomach (right) of each AIRE KO mouse. (i) 3-dimensional plots of mean frequencies of TCRα sequences in Cluster 3.2 detected in the blood (left) or stomach (right), stomach CD4⁺Teff counts, and mean signal intensities of stomach immunofluorescence. Rs, Spearman's correlation coefficient.

this issue, it is important to determine TCR repertoire specificities against stomach-derived antigens. However, a significant limitation of our approach lies in the fact that we conducted bulk-RNA-seq analysis separately for TCR α and TCR β components. As a result, we are unable to

ascertain which specific TCR α and β pair is responsible for recognizing antigens in the stomach. Moreover, we could not find potential target epitopes of the identified TCR sequences in Cluster 3.2 by searching VDJdb, a curated database of TCRs with known antigen specificities

(Shugay et al., 2018). Previously, MUCIN6 has been reported as a self-antigen involved in development of autoimmunity in AIRE KO mice (Gavanescu et al., 2007), and it is of interest to know whether identified TCR repertoires can respond to MUCIN6. However, determining the antigen specificity of TCRs based on current experimental approaches is time-consuming, and there is a significant lack of data on known TCR-peptide pairs to develop a reliable algorithm for predicting antigen specificity of any TCR (Hudson et al., 2023). Thus, it is imperative for future research to employ high-throughput experimental approaches that can concurrently identify numerous TCR-peptide pairs, exemplified by the high-resolution analysis offered by single-cell TCR repertoire analysis. Such experiments are pivotal in ensuring accurate predictions of tissue specificity within TCR repertoires.

The advantage of using a mouse model of autoimmune disease is that unlike human samples, it is easy to obtain samples from blood and peripheral organs. Especially for the purpose of this study, it would be very difficult to obtain sufficient T cells from stomachs of patients with autoimmune diseases for TCR repertoire analysis. However, TCR sequences of mice and humans are different. Clearly, there is a great need for bioinformatics tools that can predict human TCR sequences from those of mice, so that we can seamlessly translate findings from animal models to the clinic.

4 | EXPERIMENTAL PROCEDURES

4.1 | Mice

Female littermates were used in these experiments. Aire KO mice on the background of C57BL/6 were originally from the RIKEN RBC through the National Bio-Resource Project of MEXT in Japan (RBC03515: B6.Cg-Air-e<tm2Mmat>/Rbrc) mice. B6.129S7-Rag1tm1Mom/J (*Rag1*^{-/-}) were purchased from Jackson Laboratory. All mice had free access to food prior to the study. All mice were maintained under pathogen-free conditions and handled in accordance with Guidelines of the Institutional Animal Care and Use Committee of RIKEN, Yokohama Branch (2018-075).

4.2 | Cell preparation and flow cytometry

When at least one pair of WT and KO were born from the same female mouse, the mouse pair were served for

analysis when they reached 30 weeks of age. Stomach tissue was excised and immediately washed with RPMI medium. It was then minced before digestion with 1.0 mg/mL collagenase in RPMI medium (Wako) at 37°C. Supernatant containing cells was then passed through a 40- μ m filter. Cells were isolated from blood by adding 2 mL of RBC lysis buffer (Biolegend) per 100 μ L of blood collected. After incubation with RBC lysis buffer for 10–15 min at room temperature, cells were then washed with FACS buffer before antibody staining. For flow cytometry, cells were first incubated with blocking antibodies against Fc receptors (Biolegend) before staining with antibodies against TCR β , CD4, CD8, CD44, and CD62L. Dead cells were excluded by staining with 7-aminoactinomycin D. For detection of Tregs, intracellular staining was performed by incubating cells with fixation buffer for 30 min and washing with permeabilization buffer (Invitrogen) prior to incubation with blocking antibodies and antibodies against Foxp3. Cells were sorted using a FACS Aria instrument (BD) for TCR sequencing.

4.3 | TCR library preparation and sequencing

Total RNA was prepared using RNeasy Micro Kit (QIAGEN) according to the manufacturer's protocol. RNA samples with a RIN value of 8 or higher quality in the Bioanalyzer system were used for TCR repertoire analysis (7 mice for WT and 6 mice for KO). A cDNA library for TCR was prepared from RNA using a SMARTer Mouse TCR a/b Profiling Kit (Takara Bio) according to the manufacturer's protocol. To account for differences in numbers of sorted cells, RNA quantities were normalized prior to cDNA preparation. cDNA libraries of both TCR α and β were then subjected to paired-end sequencing using a Miseq (Illumina) according to the protocol for Miseq Reagent Kit v3 (Illumina).

4.4 | TCR data processing and analysis

TCR α and β sequencing data were mapped using MiTCR software (Bolotin et al., 2013). Output files from MiTCR were then converted to a format compatible with VDJtools, an analysis framework for repertoire sequencing data (Shugay et al., 2015). Diversity, clonality, CDR3 length, and significant V/J usage were calculated using VDJtools command lines. The Jaccard index of TCR repertoires between two samples was calculated by dividing the number of shared unique TCR sequences by the total number of unique TCR

sequences. The distance matrix of selected TCR sequences was generated using the `tcrdist3` python package (Dash et al., 2017), and hierarchical clustering was performed using the `hclust` function from the `stats` package in R.

4.5 | Immunofluorescence

Rag1^{-/-} tissues were snap-frozen in OCT compound. Tissues were sectioned with a cryostat (6 μm) and fixed in cold acetone for 10 min. After washing with PBS, sections were blocked with 10% normal goat serum. Sera from AIRE KO mice (100x) and control (100x) were then applied to the tissue sections and incubated for 1 h. Secondary anti-mouse antibody conjugated to Alexa-488 dye was then added along with 1 μg/mL propidium iodide (PI) and 5 μg/mL RNase A and incubated for 40 min. All images were captured using an SP8 confocal microscope (Leica).

4.6 | Statistics

Statistical analysis employed Graphpad Prism 9 software. Mann–Whitney *U* test and Student's *t*-test were used to compare means between pairs of groups, and two-way ANOVA was used to compare two groups with two independent variables. A *p*-value less than .05 was considered significant. All outliers were included in the analysis.

AUTHOR CONTRIBUTIONS

Tatsuya Ishikawa: Conceptualization, writing—original draft, investigation, formal analysis, funding acquisition, visualization. **Kenta Horie:** Investigation, formal analysis. **Yuki Takakura:** Investigation. **Houko Ohki:** Resources. **Yuya Maruyama:** Resources, writing—review & editing. **Mio Hayama:** Resources, writing—review & editing. **Maki Miyauchi:** Resources, methodology **Takahisa Miyao:** Methodology, writing—review & editing. **Naho Hagiwara:** Investigation. **Tetsuya J. Kobayashi:** Formal analysis. **Nobuko Akiyama:** Project administration, writing—review & editing, funding acquisition. **Taishin Akiyama:** Conceptualization, supervision, writing—original draft, project administration, funding acquisition.

ACKNOWLEDGMENTS

This work was supported by Grants-in-Aid for Scientific Research from JSPS (20K07332, 20H03441) (TA, NA), and CREST from Japan Science and Technology Agency (JPMJCR2011) (TA, TI). TI is supported by the establishment of university fellowships toward the creation of science technology innovation from Japan Science and Technology Agency (JPMJFS2140) and RIKEN Junior Associate Program. Computations were performed on the

NIG supercomputer at ROIS, National Institute of Genetics and HOKUSAI supercomputer at ISD, RIKEN.

ORCID

Taishin Akiyama  <https://orcid.org/0000-0002-0341-6154>

REFERENCES

- Allen, M. E., Rus, V., & Szeto, G. L. (2021). Leveraging heterogeneity in systemic lupus erythematosus for new therapies. *Trends in Molecular Medicine*, 27(2), 152–171. <https://doi.org/10.1016/j.molmed.2020.09.009>
- Anderson, M. S., Venanzi, E. S., Klein, L., Chen, Z., Berzins, S. P., Turley, S. J., Von Boehmer, H., Bronson, R., Dierich, A., Benoist, C., & Mathis, D. (2002). Projection of an immunological self shadow within the thymus by the aire protein. *Science*, 298(5597), 1395–1401. <https://doi.org/10.1126/science.1075958>
- Betterle, C., Greggio, N. A., & Volpato, M. (1998). Clinical review 93: Autoimmune polyglandular syndrome type 1. *The Journal of Clinical Endocrinology and Metabolism*, 83(4), 1049–1055. <https://doi.org/10.1210/jcem.83.4.4682>
- Bolotin, D. A., Shugay, M., Mamedov, I. Z., Putintseva, E. V., Turchaninova, M. A., Zvyagin, I. V., Britanova, O. V., & Chudakov, D. M. (2013). MiTCR: Software for T-cell receptor sequencing data analysis. *Nature Methods*, 10(9), 813–814. <https://doi.org/10.1038/nmeth.2555>
- Dash, P., Fiore-Gartland, A. J., Hertz, T., Wang, G. C., Sharma, S., Souquette, A., Crawford, J. C., Clemens, E. B., Nguyen, T. H., Kedzierska, K., La Gruta, N. L., Bradley, P., & Thomas, P. G. (2017). Quantifiable predictive features define epitope-specific T cell receptor repertoires. *Nature*, 547(7661), 89–93. <https://doi.org/10.1038/nature22383>
- Dhalla, F., Baran-Gale, J., Maio, S., Chappell, L., Hollander, G. A., & Ponting, C. P. (2020). Biologically indeterminate yet ordered promiscuous gene expression in single medullary thymic epithelial cells. *The EMBO Journal*, 39(1), e101828. <https://doi.org/10.15252/embj.2019101828>
- Gavanescu, I., Benoist, C., & Mathis, D. (2008). B cells are required for Aire-deficient mice to develop multi-organ autoinflammation: A therapeutic approach for APECED patients. *Proceedings of the National Academy of Sciences of the United States of America*, 105(35), 13009–13014. <https://doi.org/10.1073/pnas.0806874105>
- Gavanescu, I., Kessler, B., Ploegh, H., Benoist, C., & Mathis, D. (2007). Loss of Aire-dependent thymic expression of a peripheral tissue antigen renders it a target of autoimmunity. *Proceedings of the National Academy of Sciences of the United States of America*, 104(11), 4583–4587. <https://doi.org/10.1073/pnas.0700259104>
- Goldfarb, Y., Givony, T., Kadouri, N., Dobeš, J., Peligero-Cruz, C., Zalayat, I., Damari, G., Dassa, B., Ben-Dor, S., Gruper, Y., Oftedal, B. E., Bratland, E., Erichsen, M. M., Berger, A., Avin, A., Nevo, S., Haljasorg, U., Kuperman, Y., Ulman, A., & Abramson, J. (2021). Mechanistic dissection of dominant AIRE mutations in mouse models reveals AIRE autoregulation. *The Journal of Experimental Medicine*, 218(11), e20201076. <https://doi.org/10.1084/jem.20201076>

- Gray, D. H., Gavanescu, I., Benoist, C., & Mathis, D. (2007). Danger-free autoimmune disease in Aire-deficient mice. *Proceedings of the National Academy of Sciences of the United States of America*, *104*(46), 18193–18198. <https://doi.org/10.1073/pnas.0709160104>
- Hubert, F. X., Kinkel, S. A., Crewther, P. E., Cannon, P. Z., Webster, K. E., Link, M., Uibo, R., O'Bryan, M. K., Meager, A., Forehan, S. P., Smyth, G. K., Mittaz, L., Antonarakis, S. E., Peterson, P., Heath, W. R., & Scott, H. S. (2009). Aire-deficient C57BL/6 mice mimicking the common human 13-base pair deletion mutation present with only a mild autoimmune phenotype. *Journal of Immunology*, *182*(6), 3902–3918. <https://doi.org/10.4049/jimmunol.0802124>
- Hudson, D., Fernandes, R. A., Basham, M., Ogg, G., & Koochy, H. (2023). Can we predict T cell specificity with digital biology and machine learning? *Nature Reviews. Immunology*, *1–11*, 511–521. <https://doi.org/10.1038/s41577-023-00835-3>
- Jiang, W., Anderson, M. S., Bronson, R., Mathis, D., & Benoist, C. (2005). Modifier loci condition autoimmunity provoked by Aire deficiency. *The Journal of Experimental Medicine*, *202*(6), 805–815. <https://doi.org/10.1084/jem.20050693>
- Kuroda, N., Mitani, T., Takeda, N., Ishimaru, N., Arakaki, R., Hayashi, Y., Bando, Y., Izumi, K., Takahashi, T., Nomura, T., Sakaguchi, S., Ueno, T., Takahama, Y., Uchida, D., Sun, S., Kajiuira, F., Mouri, Y., Han, H., Matsushima, A., ... Matsumoto, M. (2005). Development of autoimmunity against transcriptionally unrepresed target antigen in the thymus of Aire-deficient mice. *Journal of Immunology*, *174*(4), 1862–1870. <https://doi.org/10.4049/jimmunol.174.4.1862>
- Liu, X., Zhang, W., Zhao, M., Fu, L., Liu, L., Wu, J., Luo, S., Wang, L., Wang, Z., Lin, L., Liu, Y., Wang, S., Yang, Y., Luo, L., Jiang, J., Wang, X., Tan, Y., Li, T., Zhu, B., ... Lu, Q. (2019). T cell receptor β repertoires as novel diagnostic markers for systemic lupus erythematosus and rheumatoid arthritis. *Annals of the Rheumatic Diseases*, *78*(8), 1070–1078. <https://doi.org/10.1136/annrheumdis-2019-215442>
- Lu, C., Pi, X., Xu, W., Qing, P., Tang, H., Li, Y., Zhao, Y., Liu, X., Tang, H., & Liu, Y. (2022). Clinical significance of T cell receptor repertoire in primary Sjogren's syndrome. *eBioMedicine*, *84*, 104252. <https://doi.org/10.1016/j.ebiom.2022.104252>
- Meredith, M., Zemmour, D., Mathis, D., & Benoist, C. (2015). Aire controls gene expression in the thymic epithelium with ordered stochasticity. *Nature Immunology*, *16*(9), 942–949. <https://doi.org/10.1038/ni.3247>
- Mitchell, A. M., & Michels, A. W. (2020). T cell receptor sequencing in autoimmunity. *Journal of Life Sciences*, *2*(4), 38–58. <https://doi.org/10.36069/jols/20201203>
- Moore, E., Huang, M. W., Jain, S., Chalmers, S. A., Macian, F., & Putterman, C. (2020). The T cell receptor repertoire in neuropsychiatric systemic lupus erythematosus. *Frontiers in Immunology*, *11*, 1476. <https://doi.org/10.3389/fimmu.2020.01476>
- Niki, S., Oshikawa, K., Mouri, Y., Hirota, F., Matsushima, A., Yano, M., Bando, Y., Izumi, K., Matsumoto, M., & Nakayama, K. I. (2006). Alteration of intra-pancreatic target-organ specificity by abrogation of Aire in NOD mice. *The Journal of Clinical Investigation*, *116*(5), 1292–1301. <https://doi.org/10.1172/jci26971>
- Oftedal, B. E., Ardesjö Lundgren, B., Hamm, D., Gan, P. Y., Holdsworth, S. R., Hahn, C. N., Schreiber, A. W., & Scott, H. S. (2017). T cell receptor assessment in autoimmune disease requires access to the most adjacent immunologically active organ. *Journal of Autoimmunity*, *81*, 24–33. <https://doi.org/10.1016/j.jaut.2017.03.002>
- Perheentupa, J. (1996). Autoimmune polyendocrinopathy—candidiasis—ectodermal dystrophy (APECED). *Hormone and Metabolic Research*, *28*(7), 353–356. <https://doi.org/10.1055/s-2007-979814>
- Perniola, R. (2018). Twenty years of AIRE. *Frontiers in Immunology*, *9*, 98. <https://doi.org/10.3389/fimmu.2018.00098>
- Ramsey, C., Winqvist, O., Puhakka, L., Halonen, M., Moro, A., Kämpe, O., Eskelin, P., Peltto-Huikko, M., & Peltonen, L. (2002). Aire deficient mice develop multiple features of APECED phenotype and show altered immune response. *Human Molecular Genetics*, *11*(4), 397–409. <https://doi.org/10.1093/hmg/11.4.397>
- Schatz, D. G., & Ji, Y. (2011). Recombination centres and the orchestration of V(D)J recombination. *Nature Reviews. Immunology*, *11*(4), 251–263. <https://doi.org/10.1038/nri2941>
- Shugay, M., Bagaev, D. V., Turchaninova, M. A., Bolotin, D. A., Britanova, O. V., Putintseva, E. V., Pogorelyy, M. V., Nazarov, V. I., Zvyagin, I. V., Kirgizova, V. I., Kirgizov, K. I., Skorobogatova, E. V., & Chudakov, D. M. (2015). VDJtools: Unifying post-analysis of T cell receptor repertoires. *PLoS Computational Biology*, *11*(11), e1004503. <https://doi.org/10.1371/journal.pcbi.1004503>
- Shugay, M., Bagaev, D. V., Zvyagin, I. V., Vroomans, R. M., Crawford, J. C., Dolton, G., Komech, E. A., Sycheva, A. L., Koneva, A. E., Egorov, E. S., Eliseev, A. V., Van Dyk, E., Dash, P., Attaf, M., Rius, C., Ladell, K., McLaren, J. E., Matthews, K. K., Clemens, E. B., ... Chudakov, D. M. (2018). VDJdb: A curated database of T-cell receptor sequences with known antigen specificity. *Nucleic Acids Research*, *46*(D1), D419–d427. <https://doi.org/10.1093/nar/gkx760>
- Stadinski, B. D., Shekhar, K., Gomez-Tourino, I., Jung, J., Sasaki, K., Sewell, A. K., Peakman, M., Chakraborty, A. K., & Huseby, E. S. (2016). Hydrophobic CDR3 residues promote the development of self-reactive T cells. *Nature Immunology*, *17*(8), 946–955. <https://doi.org/10.1038/ni.3491>
- Su, M. A., Giang, K., Zumer, K., Jiang, H., Oven, I., Rinn, J. L., DeVoss, J. J., Johannes, K. P., Lu, W., Gardner, J., Chang, A., Bubulya, P., Chang, H. Y., Peterlin, B. M., & Anderson, M. S. (2008). Mechanisms of an autoimmunity syndrome in mice caused by a dominant mutation in Aire. *The Journal of Clinical Investigation*, *118*(5), 1712–1726. <https://doi.org/10.1172/jci34523>
- Suzuki, M., Wiers, K. M., Klein-Gitelman, M. S., Haines, K. A., Olson, J., Onel, K. B., Passo, M. H., Singer, N. G., Tucker, L., Ying, J., Devarajan, P., & Brunner, H. I. (2008). Neutrophil gelatinase-associated lipocalin as a biomarker of disease activity in pediatric lupus nephritis. *Pediatric Nephrology*, *23*(3), 403–412. <https://doi.org/10.1007/s00467-007-0685-x>
- Venanzi, E. S., Melamed, R., Mathis, D., & Benoist, C. (2008). The variable immunological self: Genetic variation and

nongenetic noise in Aire-regulated transcription. *Proceedings of the National Academy of Sciences of the United States of America*, 105(41), 15860–15865. <https://doi.org/10.1073/pnas.0808070105>

- Wu, H., Zeng, J., Yin, J., Peng, Q., Zhao, M., & Lu, Q. (2017). Organ-specific biomarkers in lupus. *Autoimmunity Reviews*, 16(4), 391–397. <https://doi.org/10.1016/j.autrev.2017.02.011>
- Ye, X., Wang, Z., Ye, Q., Zhang, J., Huang, P., Song, J., Li, Y., Zhang, H., Song, F., Xuan, Z., & Wang, K. (2020). High-throughput sequencing-based analysis of T cell repertoire in lupus nephritis. *Frontiers in Immunology*, 11, 1618. <https://doi.org/10.3389/fimmu.2020.01618>
- Zhang, F., Gao, X., Liu, J., & Zhang, C. (2023). Biomarkers in autoimmune diseases of the central nervous system. *Frontiers in Immunology*, 14, 1111719. <https://doi.org/10.3389/fimmu.2023.1111719>

SUPPORTING INFORMATION

Additional supporting information can be found online in the Supporting Information section at the end of this article.

How to cite this article: Ishikawa, T., Horie, K., Takakura, Y., Ohki, H., Maruyama, Y., Hayama, M., Miyauchi, M., Miyao, T., Hagiwara, N., Kobayashi, T. J., Akiyama, N., & Akiyama, T. (2023). T-cell receptor repertoire analysis of CD4-positive T cells from blood and an affected organ in an autoimmune mouse model. *Genes to Cells*, 28(12), 929–941. <https://doi.org/10.1111/gtc.13079>